The Changing Nature of Hazardous Weather and implications for Transportation: Example from Oklahoma, USA

Esther D. Mullens[3], and Renee A. McPherson[1,2]

[1]DOI/USGS South Central Climate Adaptation Science Center, Norman, Oklahoma, [2]University of Oklahoma, Department of Geography and Environmental Sustainability, Norman, Oklahoma, [3]University of Florida, Department of Geography, Gainesville, FL

Supplemental Information

2.2 Climate Data

Data used for this work

Table S1: Information on the datasets used in this analysis, including historical observational gridded products and climate model data. Temporal and spatial resolutions, data sources, and variables calculated for this work are listed for each dataset.

Model and/or Observational Dataset	Temporal/Spatial resolution, and Source	Weather/Climate Variables Calculated
Topographic Weather (TopoWx)	800m, daily 1948-2012. Developed by Jared Oyler et al. (Oyler et al. 2014).	Freeze-thaw cycles
Daymet	800m, daily 1980-2016, Developed by NASA and Oak Ridge National Lab	Freeze-thaw cycles
Livneh	6.6 km, daily 1915-2011 (1950-2005 used in this project). Developed by B. Livneh et al. (Livneh et al. 2013). Available from NOAA Earth System Resources Lab (ERSL).	All
Multivariate Adaptive Constructed Analogues (MACAv2LIVNEH)	6.6 km, daily 1950-2100, emission pathways rcp4.5 and rcp8.5. Developed by Abatzoglou et al. (Abatzoglou and Brown, 2012). Models used included: *BNU-ESM, CanESM2, CCSM4, CNRM-CM5, CSIRO-Mk3-6-0, GFDL-ESM2G, HadGEM2-CC, HadGEM2-ES, inmcm4, IPSL-CM5A-LR, IPSL-CM5A-MR, MIROC5, MIROC-ESM, MIROC-ESM-CHEM, NorESM1-M*	All
Localized Constructed Analogues (LOCA)	1/16th degree (~6.6 km), daily 1950-2100, emission scenarios include rcp4.5 and rcp8.5. Developed Pierce et al. (e.g., Pierce et al. 2014). Models used were equivalent to that of MACA where available (13 models total).	All

Scenarios

Mullens and McPherson (2019) used an approach whereby climate models are distributed into groups based on the magnitude of their temperature and precipitation changes relative to the total multi-

model median changes in those categories (Fig. S1, Table S2). This was performed separately for mid-range and high emissions categories. Here, we perform a similar technique, using the MACA(v2 Livneh) and LOCA data (n=28, across 15 individual GCMs, two that were only available for MACA). We once again select models in the "Hot/Dry" (HD) and "Warm/Wet" (WW) categories, as these are likely to represent the largest deviations from the median in terms of their climate implications. Because most models are the same across the two SD methods, we include both models (one from MACA, and its LOCA equivalent where applicable taking the top two models in each category (4 projections when including the two methods). Other techniques used in the aforementioned paper apply, such as the need for any "Warm/Wet" category model to have a positive change in precipitation in the future climate, despite cases where the median of all models falls below zero (i.e., a drying of the climate).

The goal of this scenario approach is to examine whether the models in these categories show secular and/or distinctive trends when compared with the remaining sample. For example, do the WD models necessarily imply a greater magnitude of increase in extreme temperatures, or a lesser amount in extreme precipitation? While Mullens and McPherson (2019) answer this to some extent within the Southern Plains region, we include this here for the smaller spatial scale of central Oklahoma, as well as to continue to test the hypothesis as to whether we can use a smaller sample of climate models to capture a robust range of futures, rather than needing to use the entire sample. It may also be useful to the reader to see where each individual model in this sample lies with respect to its general temperature and precipitation changes in the late 21st century, as well as the extent to which MACA and LOCA differ.

It can also be helpful to examine the spatial distributions of temperature and precipitation change in the late 21st century, shown in Fig. S3 for MACA and S4 for LOCA, for the state of Oklahoma, and using RCP8.5. Ultimately the two SD methods replicate the general patterns of change similarly, though on the regional to local scales, inclusive of central Oklahoma, there are more substantial variations in the magnitudes of both variables.

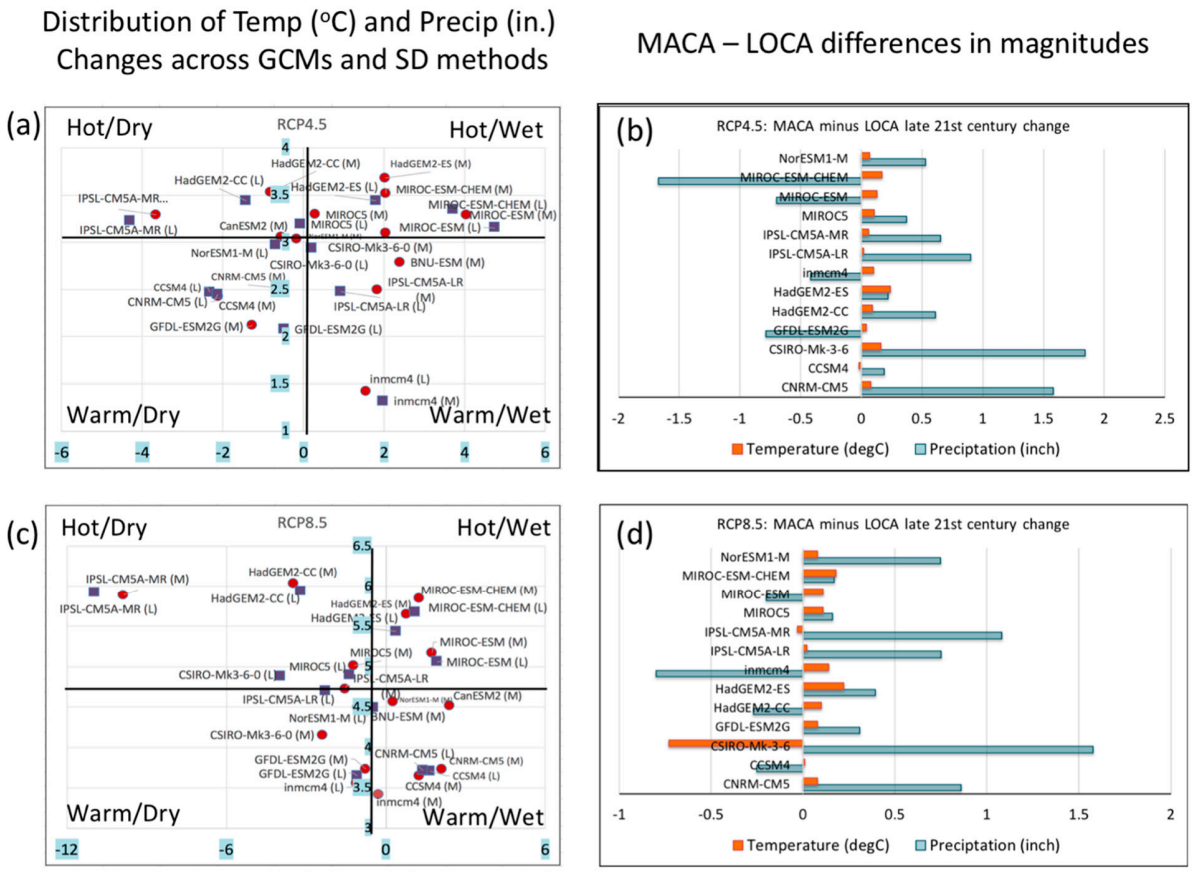

Figure S1: MACA and LOCA average precipitation change (average annual 2061-90 minus historical baseline of 1971-2000) for central Oklahoma (climate division 5) on the left – (a) RCP4.5 (midrange), (c) RCP8.5 (high). Different markers and colors identify MACA (M, red circle) from LOCA (L, purple square). The y-axis is temperature in degrees Celsius, and the x-axis is precipitation in inches. The black horizonal and vertical lines denote the median values of change for temperature and precipitation across all of the sample respectively. Panels (b) and (d) show the differences of the LOCA projections compared with MACA (i.e., MACA minus LOCA) over this period, expressed as a simple positive or negative magnitude. Note that BNU-ESM and CanESM2 are exclusive to MACA and were not analyzed.

Table S2: Models in the HD and WW categories used in this work.

Scenario	RCP4.5	RCP8.5
HD (Hot/Dry)	IPSL-CM5A-MR; HadGEM2-CC	IPSL-CM5A-MR; HadGEM2-CC
WW (Warm/Wet)	Inmcm4; IPSL-CM5A-LR; BNU-ESM (MACA only)	CCSM4; CNRM-CM5; CanESM2 (MACA only)

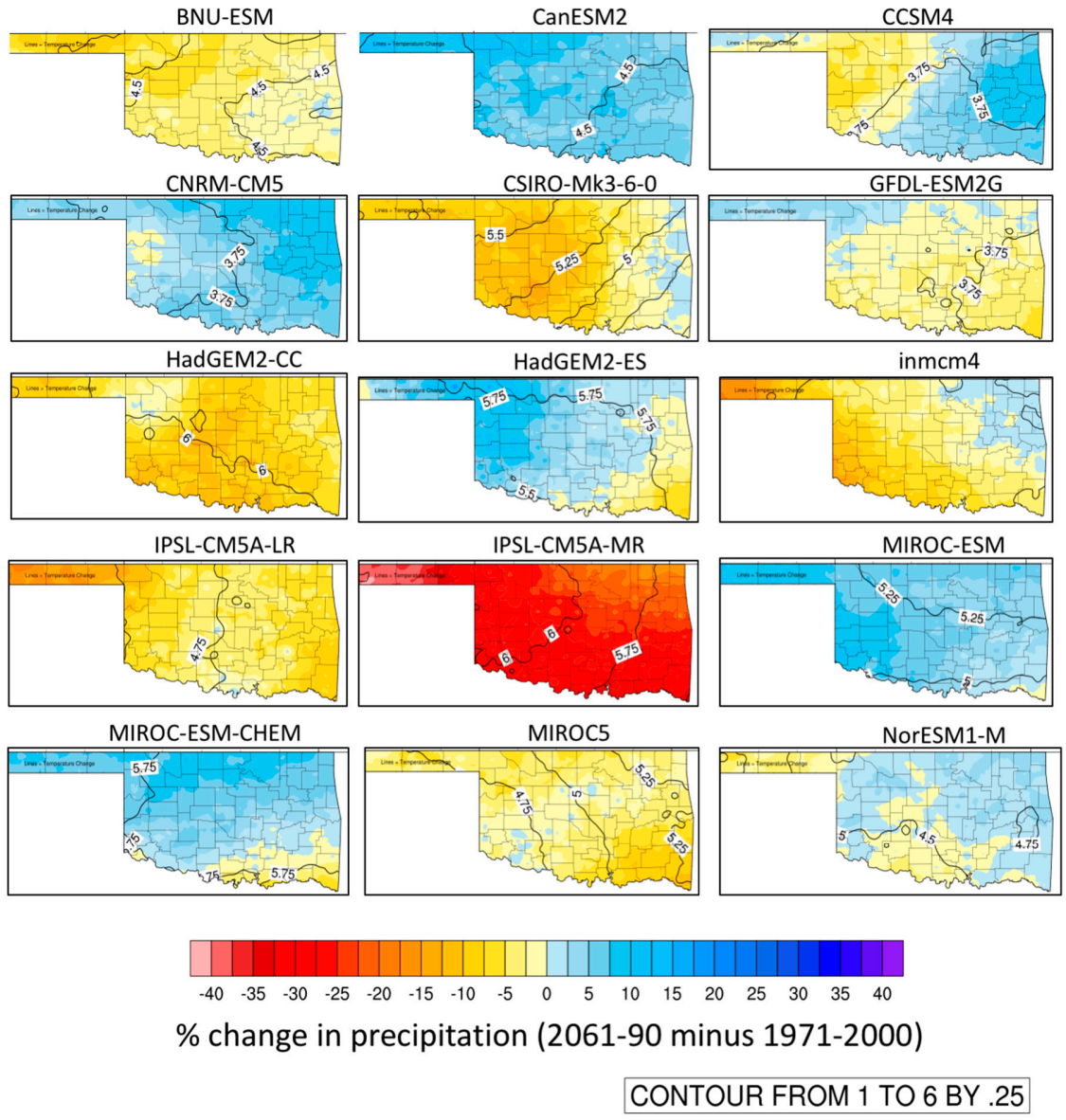

Figure S2: Spatial temperature (degC) and precipitation (%) changes from historical baseline in the late 21st century with high (RCP8.5) emissions – MACA SD method. Highlighted models indicate all those which have overlap with LOCA.

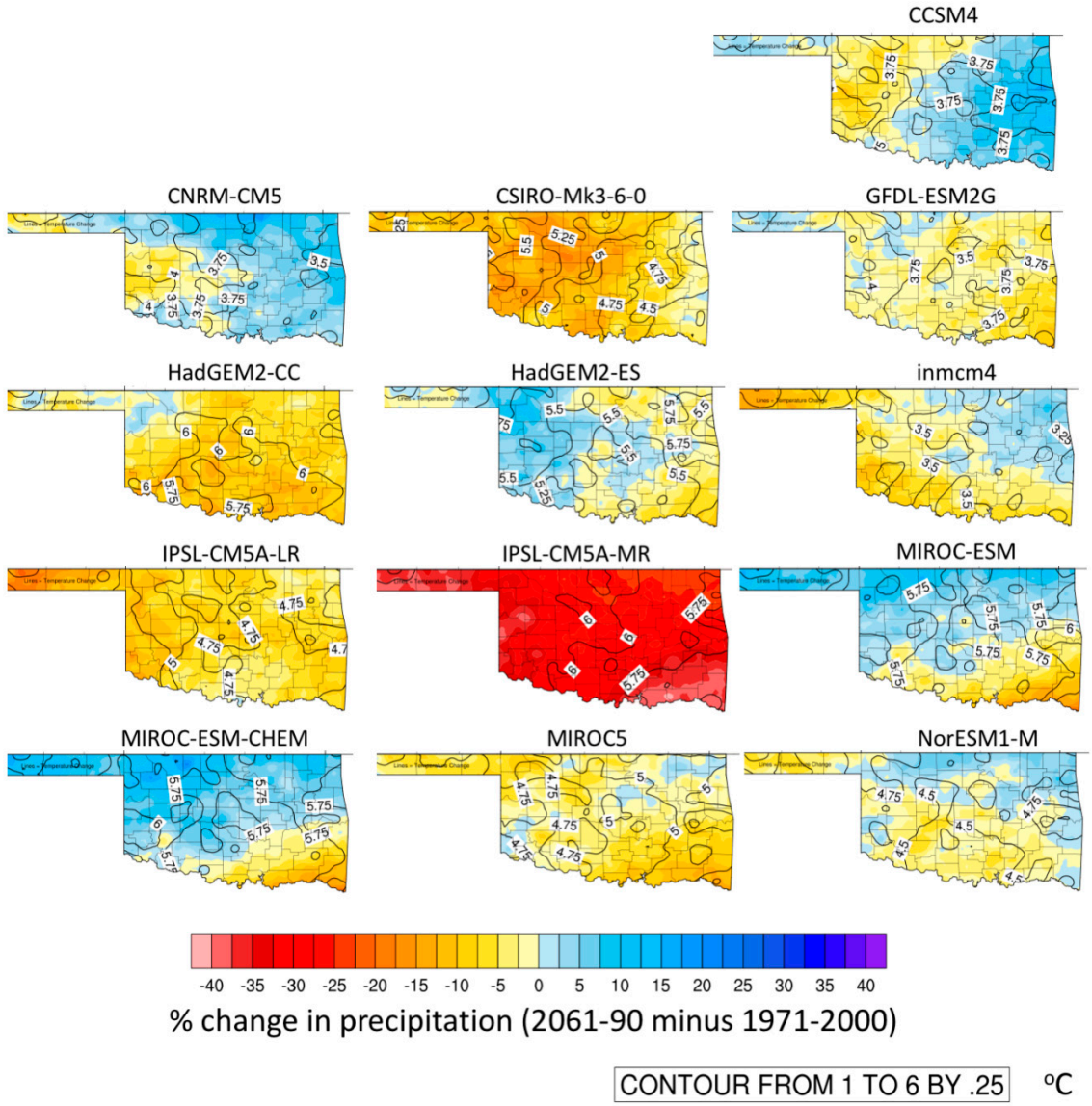

Figure S3: As Fig. S3, but for LOCA. Note the relative 'noisiness' of the temperature change projection in comparison to MACA. Identical plotting methods were applied.

3. Climate Projections

Freeze-Thaw cycles

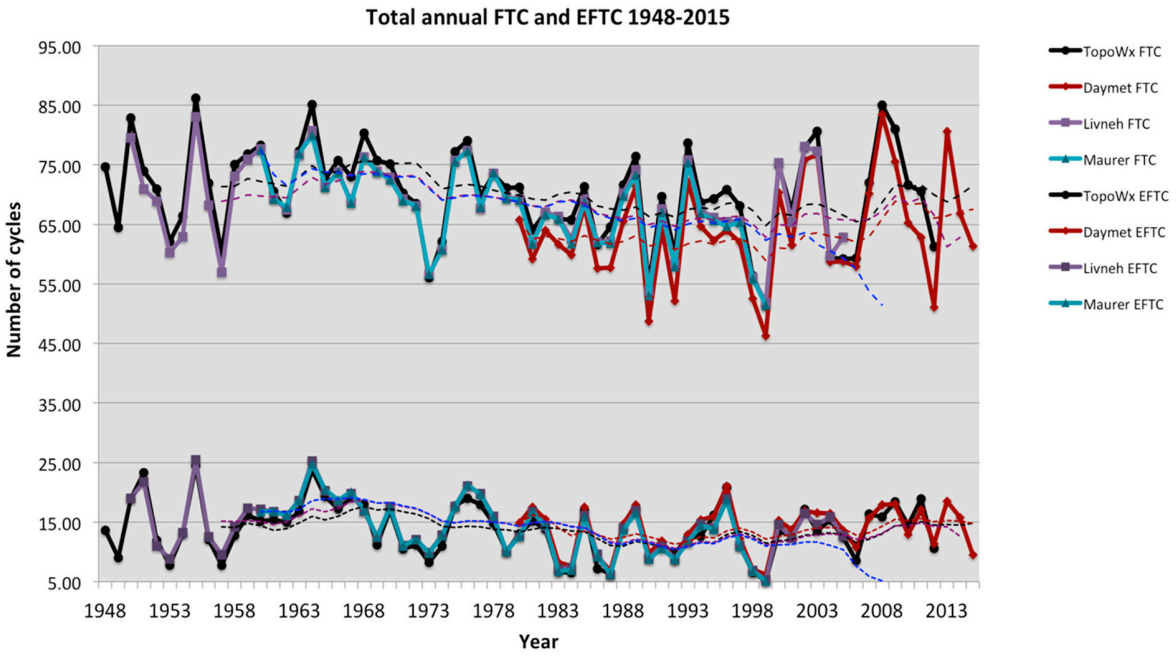

Figure S4: Historical freeze thaw cycle (FTC) trends, with magnitudes between 45-90 (days annually), and enhanced freeze thaw cycles (EFTC), with magnitudes between 5 and 25 (days annually). The time series displays four observational data products (Daymet, TopoWx, Maurer, and Livneh), regridded to a common 6.6km grid. Dashed lines are the 10-year moving averages for each (color coded to match applicable observation). Maurer data (Maurer et al. 2011) is an additional gridded observational product not used further in the main manuscript. It has a spatial resolution of 12.2 km, and temporal daily resolution from 1960-1999. It has been used to train older SD datasets using CMIP3, such as ARRM, used in Mullens and McPherson (2019).

Differences between statistically-downscaled datasets LOCA and MACAv2LIVNEH

The figure overleaf shows distributions of magnitudes for the various variables examined in section 3 of the manuscript, based on all the applicable models that have a direct match in both SD datasets (i.e., excluding BNU-ESM and CanESM2 which are only in the MACA dataset).

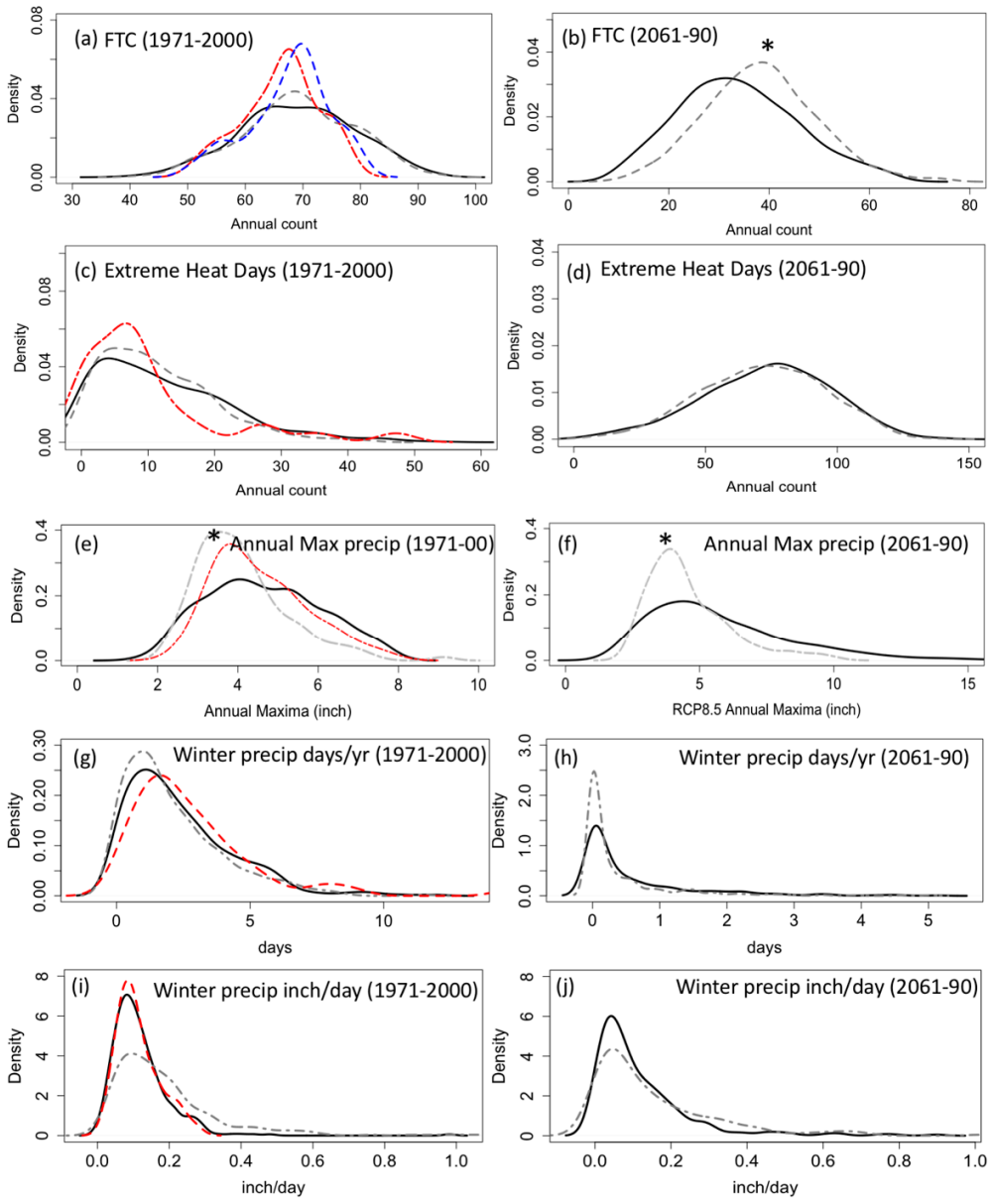

* Significance at p<=0.01 (t-test)

Figure S6: Historical (1971-2000) and late 21st century (2061-90, RCP8.5) distributions of the magnitude of key variables from section 3 – black solid line is MACA, grey dashed line is LOCA, the red dashed line is Livneh, and the blue dashed line TopoWx (FTC only). Asterisks indicate where the LOCA dataset is statistically distinct from either MACA and/or the differing x and y-axis scales.

A key finding from this brief distribution comparison is that the SD technique is most divergent between LOCA and MACA for annual maxima in precipitation, where the former has a tendency for a shorter tail, and lower mean value. LOCA in the historical period is significantly lower in the mean compared to both

MACA and Livneh. In the future projection, LOCA remains significantly lower than MACA, and the tail of the distribution is notably lengthened for MACA. Other significant differences were found between future LOCA and MACA projections for FTC, where the former showed higher counts than the latter, presumably resulting from LOCA's tendency for cooler minimum temperatures as shown in Fig. 3 of the main manuscript. The two SD approaches showed similar distributions for the majority of the remaining variables, particularly for future extreme heat and future winter precipitation frequency/intensity.

4. Discussion

4.1 Examining variance by model type, emissions, and SD data (supplement to Fig. 9).

How important are the different possible sources of projection spread (or uncertainty) relative to one another? This was the basic question that Figure 9 sought to address. The three dominant sources of spread are the emissions pathway (RCP4.5 versus RCP8.5), the models (i.e., differences between each individual projection), and the statistical downscaling method (MACA or LOCA). One additional source in the choice of extreme value distribution (EVD) was employed for return period precipitation. Our method investigates the variance of the data, with some assumptions. Variance, as the square of standard deviation, is a measure of how far a set of numbers (in this case, a climate projection) varies from its average. Thus, a greater variance implies a larger spread, which may be interpreted as higher uncertainty in the central tendency of a projection and/or less agreement between the inputs to that projection. Table S2 below describes in-brief the methods used to obtain Fig. 9.

Table S3: Description of methods used to estimate variance contributed by different factors of a climate projection.

Source of uncertainty/spread	**Method**
Model	Variance of the difference between each model from each other model. Assessed for all three reference periods and both emissions scenarios, but only average of the late-21st century with both emissions used. Only MACA model spread (n=15) evaluated.
Emissions	Variance of the difference between the RCP8.5 minus RCP4.5 projection magnitudes, for the late 21st century only.
SD technique	Variance of the difference between SD techniques (MACA minus LOCA), assessed for the three reference periods, but final value just

	for the average between the two emissions scenarios for the late 21st century.
EVD method	Variance of the difference between the 100-year return period estimates for daily precipitation (GP minus GEV), obtained for the three reference periods and both emissions pathways. Final value is average of the late 21st century two emissions pathway values.

Once the variance values had been obtained for each source, the fractional contribution to the total sum of the variances was assessed, in order to place all variables on the same scale, and to provide a measure of their relative importance in terms of the magnitude of spread. Thus, in Fig. 9, when the fractional variance is 0.1 for SD, versus 0.5 for models, as a hypothetical example, this indicates that the magnitude of the variance obtained from applying the methods in the table above showed a 5x greater variance between models, compared to that produced from the difference between the two SD methods. We focused on the future late 21st century values of variance, which for most variables represented the largest variances compared to earlier reference periods.

References (additional to main manuscript)

Maurer, E. P., Hidalgo, H. G., Das, T., Dettinger, M. D., & Cayan, D. R (2010) The utility of daily large-scale climate data in the assessment of climate change impacts on daily streamflow in California. *Hydrol. Earth Syst. Sci.*, 14, 1125–1138, https://doi.org/10.5194/hess-14-1125-2010.